

Why is Plasma Engineering in Fast Recovery Diodes by Ion Irradiation superior to Emitter Efficiency Reduction?

Oliver Humbel, Norbert Galster, Thomas Dalibor, Tobias Wikström, *Student IEEE*,
Friedhelm Bauer and Wolfgang Fichtner, *Fellow, IEEE*

Abstract-- This paper presents the comparison of two 4.5kV diodes with expanded Safe Operating Area (SOA) in terms of an expansion to higher line voltages. In order to improve the reverse recovery characteristic the excess carrier concentration close to the anode during the on-state has to be reduced. To control the injection efficiency of the anode two state of the art technologies, the reduction of the emitter doping and the ion irradiation in the p-doping region are compared in this paper. The local lifetime control technique is shown to have major advantages compared to the emitter doping reduction technique in terms of up to 50% lower switching losses at the same on-state losses due to a heavily reduced maximum reverse recovery current. Additionally, a softer switching behavior is observed for the ion-irradiated diodes. An explanation for this experimentally found behavior is provided by calibrated computer simulations.

Index terms-- local lifetime control, reduction of anode injection efficiency, P-i-N diodes, soft recovery

I. INTRODUCTION

Although new device structures for fast high power diodes have been introduced ([1], [2]), the silicon P-i-N diode is still the dominating rectifier in the field of high power conversion. However, the increasing demands for higher switching frequencies require improved diode concepts. New power switches such as the Insulated Gate Bipolar Transistor (IGBT) or the Hard Driven Gate Turn-Off Thyristor (GTO) [3] enable switching transitions at higher di/dt and dv/dt values. In this case, the P-i-N diode becomes the weakest component in a high power circuit and as such it will limit the overall performance of the circuit. This leads to new demands in the design of fast high power diodes.

The criteria for suitable diodes in various applications are a wide SOA, low static and dynamic losses, a soft recovery under all switching conditions and a low reverse recovery current [4].

Especially at low temperatures (below room temperature) and small forward current densities the soft current decay at the end of the recovery process is an important issue which is very hard to fulfill. Nowadays it is generally recognized that one of the most efficient concepts for an improved diode performance is the appropriate design of the on-state excess carrier distribution. This plasma distribution can be influenced either by varying the doping profiles or by local lifetime control [5]. The local lifetime control is realized either by exposing the diode to ion beams (helium or protons) or by doping with heavy transition metals (gold and platinum). Since the ion irradiation can be carried out after

the high temperature processes (even after metallization), this lifetime treatment is the preferred technology.

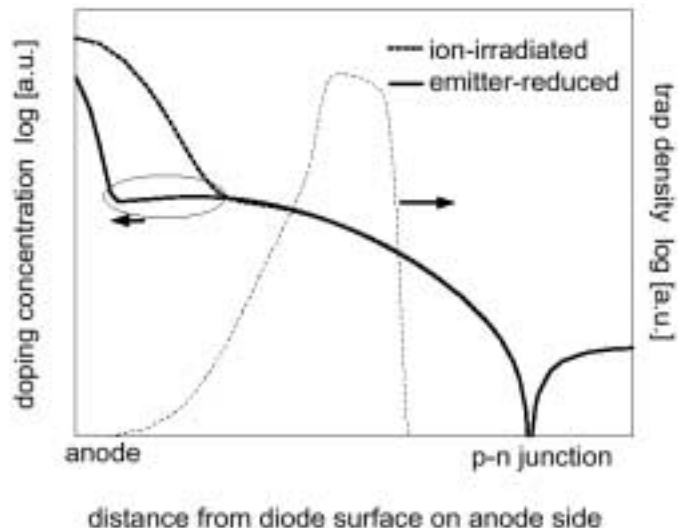


Fig. 1. Different technologies to reduce the anode injection efficiency of a 4.5kV diode: a reduced boron doping (solid) and a trap distribution in the anode resulting from a proton irradiation (dashed).

In this paper, a comparison is presented between the approach of the local lifetime control by ion irradiation and of the reduction of the anode emitter efficiency by means of reducing the emitter doping.

The paper is organized as follows: Chapter II describes the diode design and the test circuit used for the investigations in this paper. Chapter III depicts the measured and simulated results while the discussion of these results and of the different physical processes involved is presented in Chapter IV.

II. EXPERIMENTAL AND DEVICE SIMULATION

A. Diode Structures

The analyzed device is a 4.5kV presspack fast recovery diode with a base resistivity above 200 Ωcm and a total thickness of 560 μm . The anode of the device has a double profile consisting of a deep aluminum ($\sim 80\mu\text{m}$) and a shallow boron ($\sim 30\mu\text{m}$) diffusion. The injection efficiency of the anode was reduced either by reducing the B doping (both by reducing the B dose and the drive-in diffusion time) or by a proton irradiation to a depth of approx. 50 μm . The dose of the proton beam was adjusted to get exactly the same on-state voltage drop across the diode for a wide range of current densities. Both technologies are schematically shown in Fig. 1. The diodes with the reduced B doping at the anode are in the following termed "the emitter-reduced" devices. For these two different diode design concepts, 1-dimensional computer calculations with the simulator DESSIS (ISE-TCAD) [6] were performed. For the irradiated device, the distribution of the traps and their capture cross sections were

O. Humbel, T. Wikström and W. Fichtner are with the Integrated Systems Laboratory, ETH Zürich, Gloriastrasse 35, CH-9092, Switzerland, e-mail: humbel@iis.ee.ethz.ch

N. Galster, T. Dalibor and F. Bauer are with ABB Semiconductors AG, Fabrikstrasse 3, CH-5600 Lenzburg, Switzerland, e-mail: galster@chsem.mail.abb.com, dalibor@chsem.mail.abb.com

taken from work carried out previously [7] and the resulting excess carrier lifetime was calculated. The physical models of the simulator including Auger recombination, impact ionization, temperature dependent lifetime, carrier and doping concentration dependent mobility, bandgap narrowing as well as carrier-carrier scattering were calibrated with measurements (see Fig. 2). A further way to check the lifetime calibration was given by Free Carrier Absorption measurements (FCA) done at the Royal Institute of Technology in Stockholm [8].

B. Test Circuit

The reverse recovery behavior of the diodes has been analyzed in an Undeland/McMurray circuit. This type of resistive switching is realized for diodes in applications like the Undeland snubbers where the active switch is typically a GTO. The recovery of the diode in a resistive switching circuit is controlled by the turn-on behavior of the switch. This means that the rise of current (di/dt) is determined by the time dependent resistor of the switch (R_t) rather than by the stray inductance L_s (see Fig. 3) [9]. Since the inductance in the McMurray circuit is comparable to the stray inductance in IGBT-modules, this circuit is also an adequate test environment for IGBT freewheeling diodes.

For the simulations the experimental measurement set-up was simplified and implemented in a mixed mode circuit simulation. In order to save calculation time the GTO was replaced by a time dependent resistor with an exponential decay. Fig. 2 shows a comparison of the simulated and measured voltage and current density waveforms during reverse recovery for an unirradiated 4.5kV diode with a high

injection efficiency anode. The waveforms of the calibrated simulation agree very well with the measurement. In addition, FCA measurements were used to illustrate the physical processes and to extract lifetime properties of the fabricated devices. In the open-circuit decay (OCD) [10] the on-state excess carrier distribution ($t=0\mu s$) is followed by a carrier decay, which is given only by recombination and diffusion, i.e. without current through the contacts (see explanation in chapter III.A. and Figs. 4 and 5). To obtain the static losses of the different devices the forward I-V curves were measured on an industrial diode tester (LEM Diode Tester type DS5060).

III. RESULTS

A. Measurements

Figures 4 and 5 illustrate the OCD of the excess carrier distribution for the two types of diodes. The emitter-reduced diode in Fig. 4 shows the expected carrier concentration reduction close to the anode ($x=10\mu m$ at $t=0\mu s$) and a homogeneous decay of the carrier concentration (for $t>0\mu s$) due to the nearly constant lifetime throughout the device. In contrast, the ion-irradiated diode (Fig. 5) has an anode with a high emitter efficiency; in this case the on-state plasma reduction ($t=0\mu s$) is reached by a higher recombination rate near the p-n junction ($x\sim 80\mu m$).

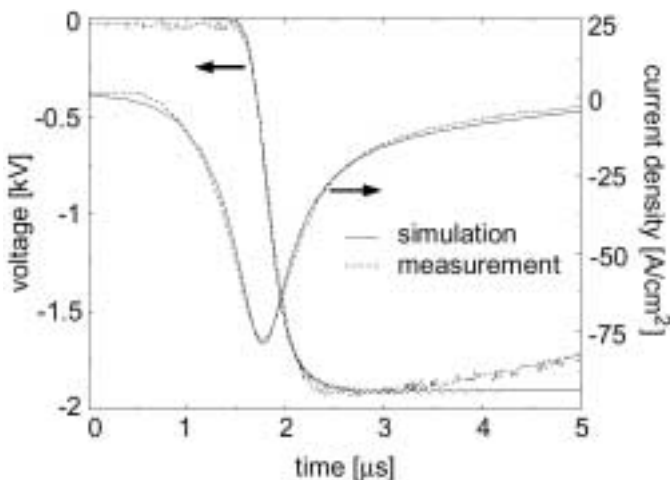


Fig. 2 Simulated (solid) and measured (dashed) reverse recovery characteristic of an unirradiated 4.5kV diode with high injection efficiency of the anode.

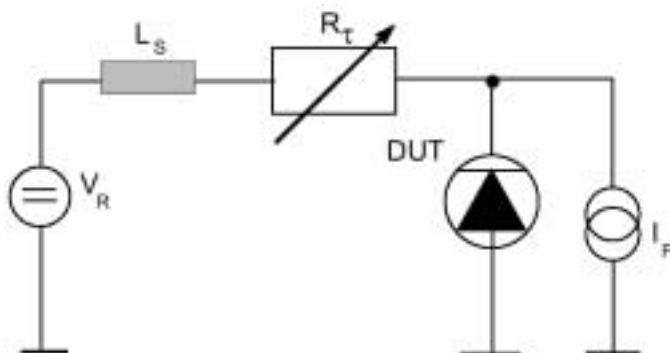


Fig. 3 Snubberless Undeland/McMurray, resistive switching circuit

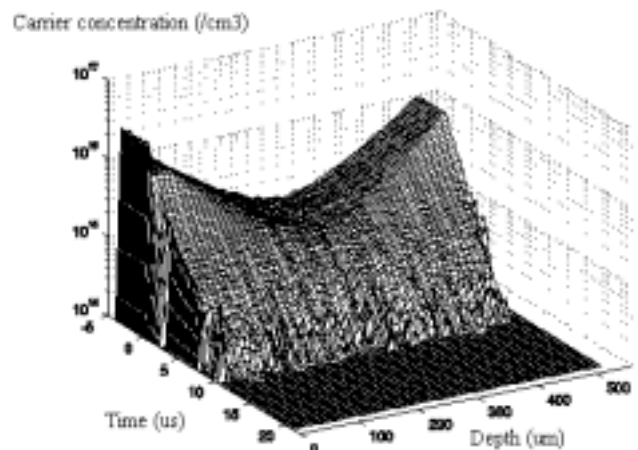


Fig. 4. Free Carrier Absorption (FCA) measurement of the emitter-reduced device at a forward current density of $100A/cm^2$. For $t<0_s$ the on-state carrier distribution is shown, for $t>0_s$ the open circuit decay.

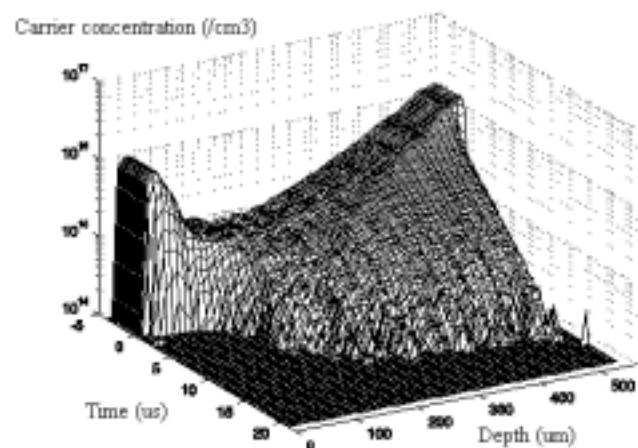


Fig. 5 FCA measurement of the proton-irradiated device at a forward current density of $100A/cm^2$. For $t<0_s$ the on-state carrier distribution is shown, for $t>0_s$ the open circuit decay.

Local lifetime control results in a faster decay of the carrier concentration at the p-n junction ($x \sim 80\mu\text{m}$) and a slower one close to the cathode ($x > 300\mu\text{m}$) compared to the emitter-reduced diode.

As described in chapter II.A the dose of the proton irradiation was chosen to get the same static losses for the

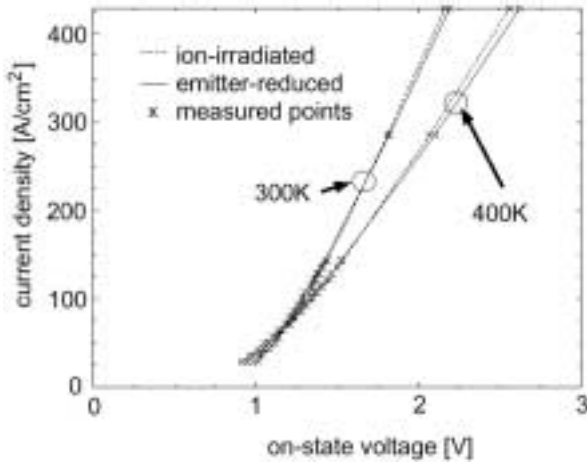


Fig. 6. Measured J-V curves of the two different diodes at 300K and 400K.

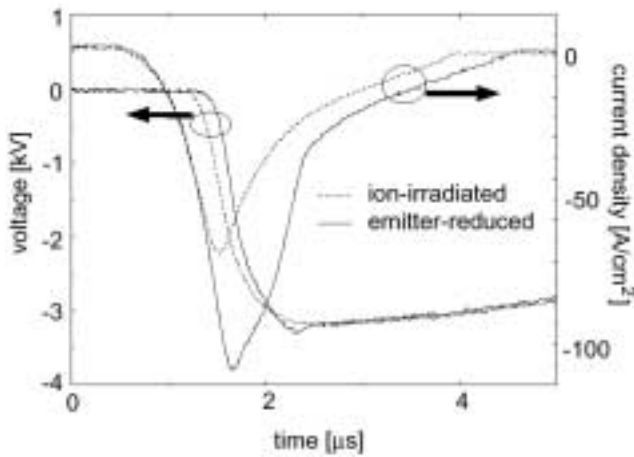


Fig. 7 Measured reverse recovery characteristics in an Undeland/McMurray-circuit at 400K with a forward current density of $2\text{A}/\text{cm}^2$ and a line voltage of 3100V . The maximum reverse recovery current density of the ion-irradiated device is reduced by $30\text{A}/\text{cm}^2$ of the value of the emitter-reduced diode.

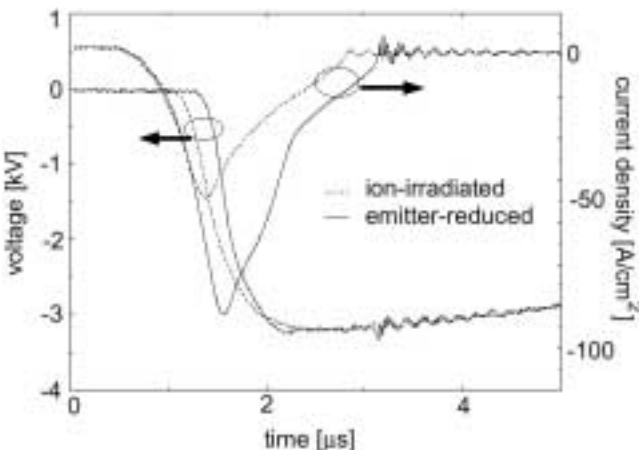


Fig. 8. Measured reverse recovery characteristics in an Undeland/McMurray circuit at 300K with a forward current density of $2\text{A}/\text{cm}^2$ and a line voltage of 3100V . The emitter-reduced diode shows harder current snapping at $3.1\mu\text{s}$.

ion-irradiated device as for the emitter-reduced diode. The J-V curves in Fig. 6 show that the two different diodes have the same on-state characteristic and that the temperature dependence of the curves is similar, e.g. the crossing points [11] for the two temperatures are the same for both diodes.

Figure 7 illustrates the reverse recovery characteristics in an Undeland/McMurray circuit for the two different diodes at a temperature of 400K . Snap-off of the diode current is most likely to occur at low forward current densities and high line voltages. In order to see the differences in softness during the tail phase, a very small current density of $2\text{A}/\text{cm}^2$ and a high line voltage of 3100V were chosen. For the ion-irradiated device a reduction of more than $30\text{A}/\text{cm}^2$ in the maximum reverse recovery current density (I_{rr}) is observed. This results in a 50% decrease in the peak power density, mainly due to the slower rise of the reverse voltage over the device. The higher peak power for the emitter-reduced diode is accompanied by the onset of impact ionization shortly after I_{rr} is reached ($t=2\mu\text{s}$). The extracted charge Q_{rr} during the recovery process differs by about 55% between the ion-irradiated and the emitter-reduced diode. At 300K the comparison shows the different softness behavior of the devices (Fig. 8) with the same switching parameters as for the 400K measurements the ion-irradiated element has a soft current decay while the emitter-reduced one shows a significant snap-back, which is accompanied by large voltage oscillations at the end of the tail phase current. Additionally the peak power density is reduced to 46% and the extracted charge during turn-off is limited to 55% of the value of the emitter-reduced diode.

B. Simulations

Figure 9 displays simulated J-V curves at 300K showing equal on-state voltage drops for both types of diode technologies in agreement with the measurements (see Fig. 6). In Fig. 10 the free charge carrier distributions for current densities of 1 and $10\text{A}/\text{cm}^2$ are shown for both diodes. In the proton-irradiated diode a significantly lower plasma density can be seen close to the junction ($\sim 80\mu\text{m}$) for low current densities as compared to the emitter-reduced one. The difference in carrier concentration is approximately 30% between 80 and $300\mu\text{m}$ at a current density of $1\text{A}/\text{cm}^2$. At the proton-induced trap density maximum ($\sim 50\mu\text{m}$) the excess carrier distribution exhibits a sharp knee (arrow in Fig. 10). In the simulation a conversion from hole- to electron-current can be seen in this region. Fig. 11 illustrates an increase of the hole current density close to the anode of almost a factor of two for the ion-irradiated diode as compared to the emitter-reduced device at current densities of $30, 55$ and $85\text{A}/\text{cm}^2$. The corresponding electron current density shows a sharp decrease around $50\mu\text{m}$ in case of the ion-irradiated device (Fig. 12). The proton-irradiated diodes have the same voltage drop, e.g. the same static losses, but a significantly reduced excess carrier concentration at the p-n junction for small current densities as compared to the emitter-reduced devices.

The impact of the different on-state plasma distributions for the two types of diodes on the dynamic reverse recovery characteristics is simulated in the Undeland/McMurray circuit discussed in chapter II.B (see Fig. 2). Because of missing damping effects in the simulated circuit the current snap-off occurs at lower line voltages and higher forward current densities. For this reason, Fig. 13 shows reverse recovery waveforms at 400K for both diodes

with a forward current density of 11 A/cm^2 and a line voltage of 2800 V . The main difference between the two types of diodes is the earlier voltage rise and the smaller maximum reverse recovery current density of the ion-irradiated device

in agreement with the measurements. In Fig. 14 the same recovery process was simulated at a temperature of 300 K . Like in the measurement shown in Fig. 8 the tail phase current of the emitter-reduced diode has a current snap-off at about $4.2 \mu\text{s}$.

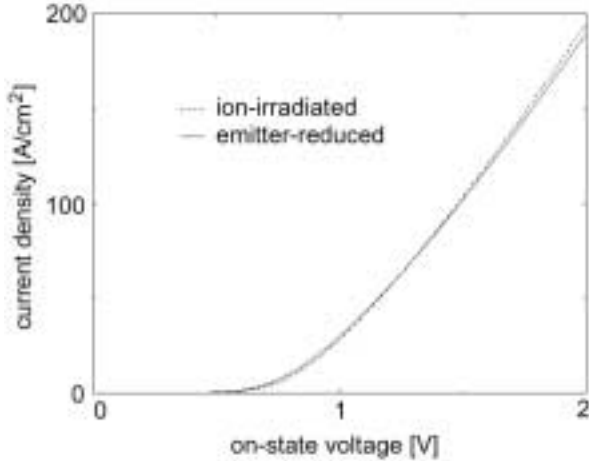


Fig. 9. Simulated J-V curves of the two different diodes at 300 K .

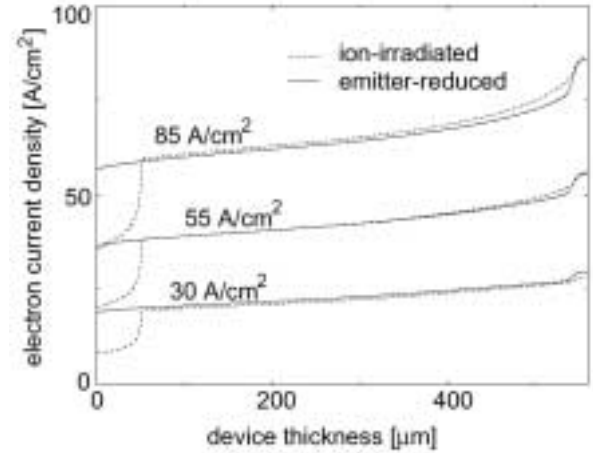


Fig. 12. Simulated electron current density for current densities of $30, 55$ and 85 A/cm^2 for the ion-irradiated (dashed lines) and the emitter-reduced (solid lines) diode. At a depth of $50 \mu\text{m}$ where the traps of the proton-irradiation are located, the electron current density is decreased for the ion-irradiated diode.

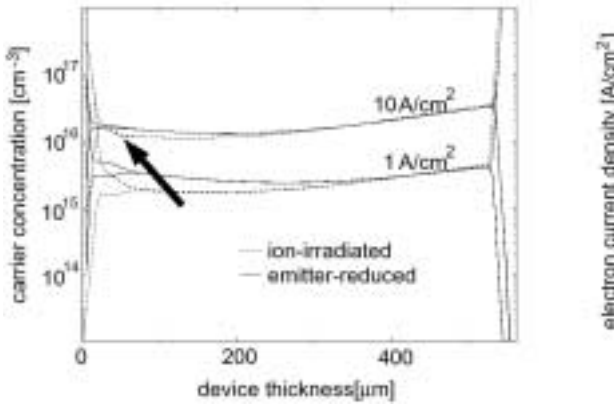


Fig. 10. Simulated carrier distribution at two current densities 1 and 10 A/cm^2 , respectively, for the ion-irradiated (dashed lines) and for the emitter-reduced (solid lines) diode.

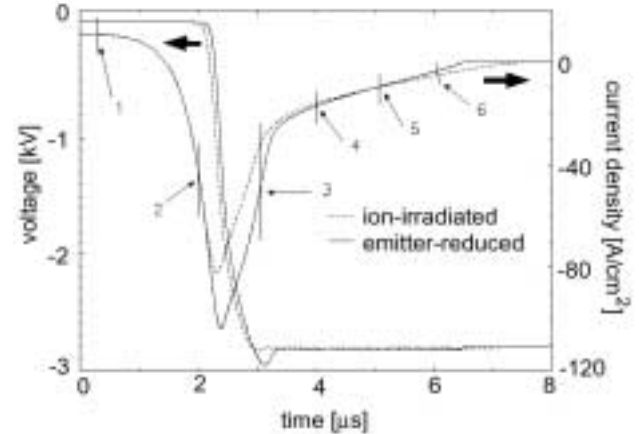


Fig. 13. Simulated reverse recovery characteristics in an Undeland/McMurray circuit at 400 K with a forward current density of 11 A/cm^2 and a line voltage of 2800 V . For the different points of time (1-6) the hole distribution is shown in Fig. 15.

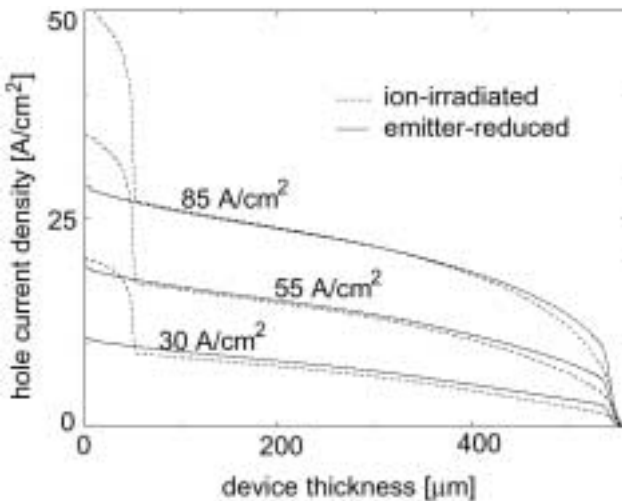


Fig. 11. Simulated hole current density for current densities of $30, 55$ and 85 A/cm^2 for the ion-irradiated (dashed lines) and the emitter-reduced (solid lines) diode. At a depth of $50 \mu\text{m}$ where the traps of the proton-irradiation are located, the hole current density is increased for the ion-irradiated diode.

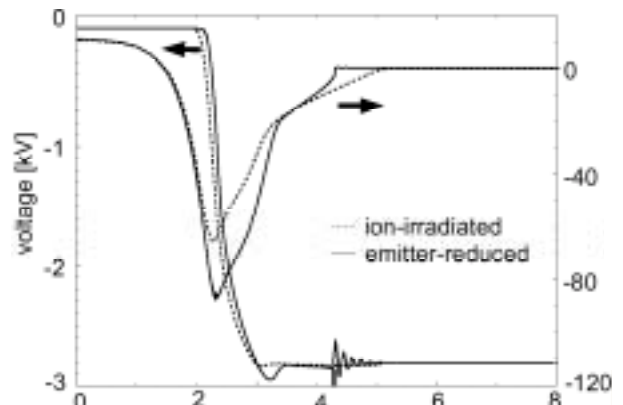


Fig. 14. Simulated reverse recovery characteristics in an Undeland/McMurray circuit at 300 K with a forward current density of 11 A/cm^2 and a line voltage of 2800 V .

IV. DISCUSSION

Both measurements and simulations show that the ion-irradiated device has a better trade-off between static and dynamic losses than the emitter-reduced one. For devices with a homogeneous lifetime like the emitter-reduced device, the optimum plasma distribution for an optimized trade-off between on-state and turn-off losses is flat. Unfortunately, such a distribution leads to very snappy behavior of the reverse recovery current.

Improving the softness and reducing the maximum reverse recovery current requires a lower excess carrier concentration at the p-n junction as compared to the n + -n - junction. This is realized for both the ion-irradiated and the emitter-reduced devices, but to different extents.

In order to explain why the on-state losses are equal for both types of diodes, although the overall plasma density is lower for the proton-irradiated diode, one has to distinguish between the drift current (electric field is the driving force) and the diffusion current (the gradient of the plasma distribution is the driving force). Due to the conversion of hole- to electron-current in the area of high recombination (Figs. 11 and 12) additional diffusion of excess carriers because of steep gradients lowers the on-state voltage in the ion-irradiated diode. Up to a depth of approx. 50µm of the device, the gradient of the carrier distribution enhances the current carried by holes. For low current densities this will lead to a smaller excess carrier concentration at the same amount of static losses.

In the dynamic turn-off characteristic this difference in the on-state plasma level leads to a smaller t_{rr} and a softer turn-off behavior for the proton-irradiated diode. Due to the decreasing lifetime at lower temperatures the excess carrier concentration at room temperature is reduced and the current snap-off oscillations occur more significantly compared to 400K (see Figs. 7 and 8).

For different points of time the simulated hole

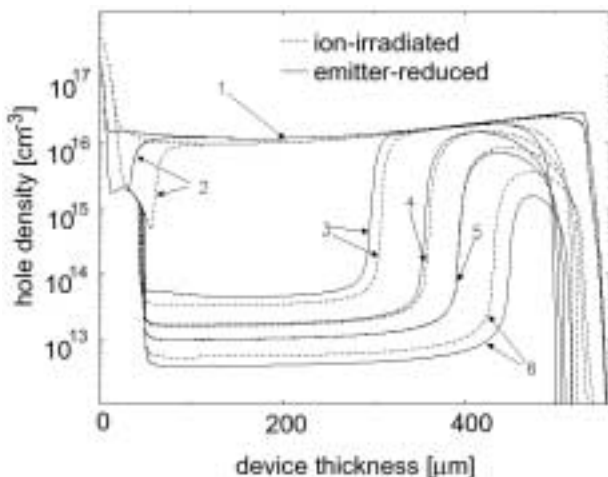


Fig. 15. Simulated hole density distribution during the reverse recovery process shown in Fig. 13. The ion-irradiated device shows a faster depletion of the p-n junction (point 2, 3) and more plasma towards the end of the recovery process (point 6).

density distribution during the reverse recovery process is plotted in Fig. 15. The lower plasma concentration at the p-n junction (around 80µm) combined with an additional recombination process due to the ion-induced traps leads to a faster depletion of the anode-side space charge region for the

proton-irradiated diode in the beginning of the turn-off process (time point 2 and 3). As the diode reverse blocking voltage is established faster, the reverse recovery current is correspondingly limited earlier, i.e. a lower t_{rr} is obtained. In addition, the depletion region at the n + -n - junction, having less time to expand, is smaller at every time point for the ion-irradiated diode. At time point 5, the reverse recovery current is again comparable for the two devices, although less charge has been extracted from the ion-irradiated diode. The remaining charge is now helping to keep the two depleted zones from meeting allowing a soft recovery of the ion-irradiated diode; i.e. the closer the remaining carriers are located to the cathode the softer the device behaves. At time point 6, the space charge region of the emitter-reduced diode has passed that one of the ion-irradiated device due to the lower amount of charge left in the emitter-reduced diode.

It can therefore be concluded that the lower on-state excess carrier distribution of the proton-irradiated diode leads to a faster establishment of the reverse voltage over the diode and consequently, to a lower reverse recovery current maximum. In addition, a softer reverse recovery behavior is achieved due to the larger amount of stored charge, which remains in the diode during the tail current stage.

A broader range of forward current densities with related maximum t_{rr} is shown in Fig. 16. Differences in the maximum reverse recovery current density up to 45% between the two technologies can be identified. Above forward current densities of 5A/cm² Impact ionization dominates the recovery characteristic including the maximum t_{rr} .

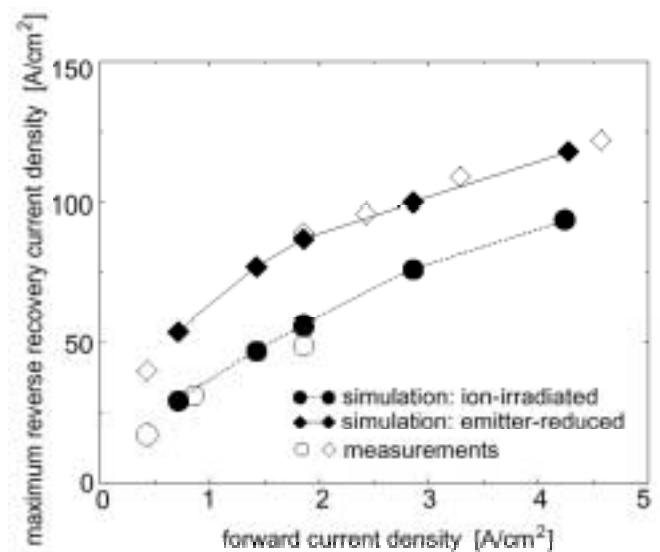


Fig. 16. Simulated and measured dependency of the maximum reverse recovery current density on the forward current density. The emitter-reduced (solid) and the ion-irradiated (dashed) diodes were recovered against a line voltage of 3100V at 300K.

V. SUMMARY

Two different diode technologies to enhance the reverse recovery performance especially in the demanding conditions of small forward currents, low temperatures and high line voltages, the emitter reduction and the ion irradiation were compared in this paper on a 4.5kVdiode. In experimental studies the ion-irradiated device shows a much better trade-off between static and dynamic losses. At

identical static losses the maximum reverse recovery current is reduced up to 50% compared to the emitter-reduced structures. Additionally, a softer reverse recovery process at increased line voltage enhances the SOA of the proton-irradiated diode.

The physical analysis of the investigated technologies were performed by calibrated mixed mode computer simulations. It is shown that the ion-irradiated devices have an optimized on-state excess carrier distribution which leads to a faster establishment of the blocking voltage, a lower reverse recovery current and a softer tail phase behavior at the commutation process as compared to the emitter-reduced devices.

ACKNOWLEDGEMENTS

The authors wish to thank Stefan Müller and Kurt Haas of the Q&R department of ABB Semiconductors AG for their help in device testing.

REFERENCES

- [1] H. Schlangenotto, J. Serafin, F. Sawitzki and H Maeder, "Improved recovery of fast power diodes with self-adjusting p emitter efficiency", *Electron Dev. Lett.*, vol. 10, pp. 322, 1989
- [2] S. Sawant, B. Baliga, "A Comparative Study of High Voltage (4kV) Power Rectifiers PiN/MPS/SSD/SPEED", *Proc. ISPSD 99, Toronto*, pp. 153, 1999
- [3] H. Grüning, B. Oedegard, J. Rees, A. Weber, E. Carroll and S. Eicher, "High-power hard-driven GTO module for 4.5kV/3kA snubberless operation", *Proc. PCIM 96 Europe*, pp. 169-183, 1996
- [4] N. Galster, M. Frecker, E. Carroll, J. Vobecky and P. Hazdra, "Application-Specific Fast-Recovery Diode: Design and Performance", *Proc. PCIM, Tokyo 98*, pp. 69, 1997
- [5] J. Vobecky, P. Hazdra, N. Galster, E. Carroll, "Free-wheeling diodes with improved reverse-recovery by combined electron and proton irradiation", *Proc. PEMC'98*, pp.1-22, 1998
- [6] R. Escoffier, W. Fichtner, D. Fokkema, E. Lyumkis, O. Penzin, B. Polsky, A. Schenk and B. Schmithüsen, "DESSIS 5.0 Manual", ISE Integrated Systems Engineering AG, CH - Zürich, 1996
- [7] J. Vobecky, P. Hazdra, "Simulation of power diodes", Internal Report ABB Semiconductors, Prague, 1996
- [8] M. Lundqvist, H. Bleichner, E. Nordlander, "An Optical System for Bilateral Recombination-Radiation Diagnostics of the Carrier Redistribution in Switching Power Devices", *IEEE Transaction on Instrumentation and Measurement*, vol. 40, no. 6, pp. 956, 1991
- [9] O. Humbel, N. Galster, F. Bauer, W. Fichtner, "4.5kV-Fast- Diodes with Expanded SOA Using a Multi-Energy Proton Lifetime Control Technique", *Proc. ISPSD 99, Toronto*, pp. 121, 1999
- [10] M. Rosling, H. Bleichner, M. Lundqvist and E. Nordlander, "A Novel Technique for the Simultaneous Measurement of Ambipolar Carrier Lifetime and Diffusion Coefficient in Silicon", *Solid-State Electronics*, vol. 38, no.9, pp. 1223, 1992
- [11] J. Vobecky, P. Hazdra, O. Humbel, N. Galster, "Crossing Point Current of Power P-i-N Diodes: Impact of Lifetime Treatment", *Proc. MIEL, Nis*, 1999